Driver Design for Practical Implementation of the Haptic Feedback with Ultrasonic Surface

Anis Kaci, Frédéric Giraud

Driver Design for Practical Implementation of the Haptic Feedback with Ultrasonic Surface

Kaci Anis
University of Lille)
Villeneuve d'Ascq, France
anis.kaci@univ-lille.fr

Giraud Frédéric
University of Lille)
Villeneuve d'Ascq, France
frederic.giraud@univ-lille.fr

***Abstract*—This paper presents a practical implementation of a driver that supplies power to an ultrasonic haptic surface. In the proposed 2-stage topology, a BOOST converter first modulates a high voltage DC Bus to produce the haptic feedback. A second stage converts the DC Bus voltage to an AC one at the resonant frequency of the tactile plate. We demonstrate that a commercial product originally designed to produce haptic feedback on a low frequency piezoelectric actuator can be used with a haptic surface which resonant frequency is 60kHz, without transformer. This is why, we believe that this topology will help to introduce more ultrasonic haptic surfaces into consumer products.**

***Index Terms*—Piezoelectricity, haptic surface, tactile feedback**

I. Introduction

Haptic feedback is introduced into consumer products in order to enrich the physical interactions between users and machines. This is achieved with actuators that create vibrations of handheld devices [1], in order to convey information like alerts or transient events. Among the possible actuators technology that can be used in this domain, piezoelectric actuators outperform magnetic ones in terms of expressiveness [2]. However, they require high voltage to operate, typically 100V, which complicates the electronic architecture that energizes them. But recently, commercial haptic drivers were introduced to easily operate a piezoelectric actuator at a frequency up to 250Hz and up to 100V voltage amplitude, by exploiting the boost architecture [3].

For the specific case of touch interfaces, which require to produce haptic feedback on transparent surfaces, the *Haptic Surfaces* were developped [4]. A variety of physical phenomenon were exploited to create a programmable tactile stimulation and to exploit tactile illusions. For instance, it is possible to render the illusion of touching a textured surface on a flat and hard touchscreen, by modulating the friction between a user's fingertip and the surface. This can be achieved by exploiting electrostatic forces [5], or by propagating ultrasonic vibrations on the surface to reduce the friction, a phenomenon called *Active lubrication* [6].

In that second example, piezoelectric actuators are used to create a vibration at high operating frequency ($\sim$ 50kHz) and low vibration amplitude ($\sim$ 1μm). Since the actuators are located at the periphery of the tactile interface, this solution has the advantage to be compatible with the sensing capabilities of touchscreens [7]. In spite of design optimization that allows low power consumption [8], the frequency requirement do not fall into the specifications of the aforementioned haptic drivers. As a result, specific electronic drivers need to be designed for each haptic surface, as well as specific development tools and framework (like haptic waveform builders, USB controllers, ...).

Identify applicable funding agency here. If none, delete this.

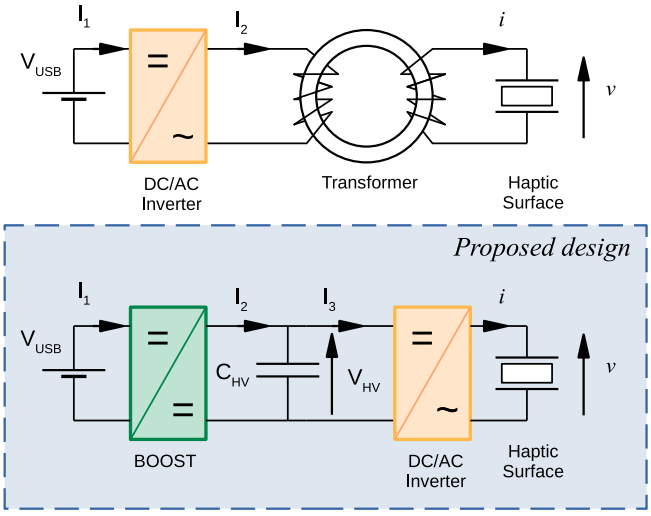

Fig. 1. Driver topology of ultrasonic haptic surface; top: state of the art, bottom: proposed design.

In this paper, we describe a new driver topology that is compatible with the commercial piezoelectric haptic drivers. The design rules are given in the following section, while the energetic performances are evaluated in the third section. Finally, we show how to use the haptic capabilities of the commercial haptic driver to drive a friction reduction based haptic surface.

II. Design principle

A. Energy conversion in the driver

Generally, the drivers of ultrasonic tactile interfaces rely on a two stages voltage transformation. At first, an inverter converts a low DC voltage into an AC one, at the operating frequency of the stimulator. Then, a transformer steps up the

voltage to meet the requirements of the interface [9], [10]. To modulate the friction, the voltage amplitude is modulated by the inverter.

In the proposed driver topology depicted fig. 1, the inverter creates an AC voltage at fixed frequency, and is placed after a boost converter that fulfills two functions: first, it steps up the low voltage bus to a higher one named High Voltage (HV) bus in the remaining of the paper; second, it modulates the HV bus to modulate the friction.

This topology allows us to use a commercial haptic driver for the boost converter, and to remove the transformer. The design however relies on the calculation of the DC bus voltage capacitance C_{HV} (see figure 1). Indeed, if C_{HV} is too high, the BOOST converter cannot dynamically modulate the HV bus voltage. If it's too low, the DC bus voltage shows unwanted ripples. A compromise must be found, and is presented in the next section.

B. Calculation of the High Voltage Bus Capacitor

The piezoelectric actuators that produce the ultrasonic vibration of the plate show a capacitive behaviour, and the Butterworth-Von Dyke model presented figure 2 is widely used for the description of the electrical behaviour [11]. It consists in a capacitance C_0 is in parallel with the *motional* branch (R_m, C_m, L_m).

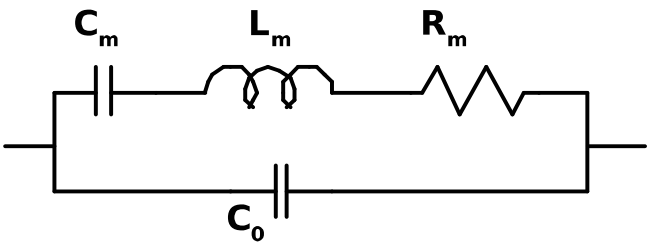

Fig. 2. The Butterworth Van Dyke equivalent circuit for a piezoelectric resonator.

The actuators require a high voltage v and a high current i, both at high frequency f; the power $p(t) = vi$ can be positive or negative, as depicted figure 3.

Therefore, the power that flows to the actuators is not constant, but is alternating at twice the frequency of the vibration. If the power is positive, the capacitor C_{HV} discharge into the inverter. Conversely, when p is negative, the inverter extracts power from the actuators and sends it back to C_{HV}. As a result, C_{HV} can be seen as a transitory reserve of energy E which can be written as:

$$E = \frac{1}{2} C_{HV} V_{HV}^2 \tag{1}$$

Therefore, the voltage V_{HV} will oscillate around a mean value V_0, increasing when $p < 0$ because C_{HV} retrieves energy, and decreasing when $p > 0$. The bigger C_{HV} the smaller the oscillations.

For sake of simplicity, without changing the conclusions of the paper, we assume that the inverter has no power losses and voltage and current are phased shifted by ninety degrees,

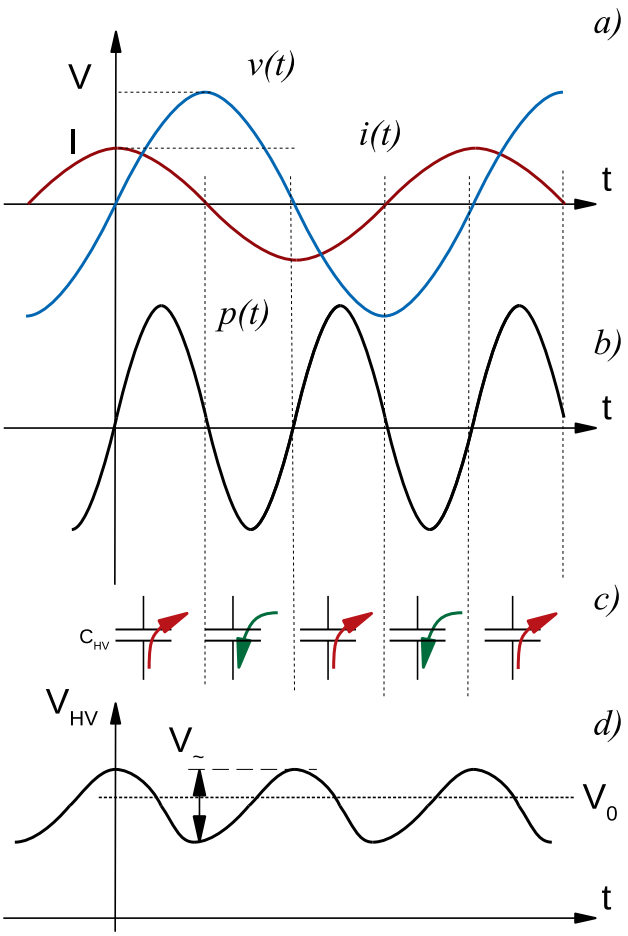

Fig. 3. Behavior of the HV bus. a) Voltage v current i and b) power p required by an ultrasonic tactile plate c) the charge/discharge cycles of C_{HV} and d) the HV bus voltage V_{HV}.

which means that we consider the capacitive behaviour only. We write:

$$v = V sin(2\pi f t) \qquad i = I cos(2\pi f t) \tag{2}$$

with f the operating frequency of the plate, and

$$p = -\frac{dE}{dt} \tag{3}$$

These assumptions allow us to calculate the amplitude of the oscillations of V_{HV}. Indeed, by introducing 1 and 2 into 3, we can calculate the voltage V_{HV} as a function of time:

$$V_{HV} = \sqrt{V_0^2 + \frac{VI}{4\pi C_{HV} f} cos(2\pi f t)} \tag{4}$$

The amplitude of the oscillations $V_\sim$ of V_{HV} can be calculated from the maximum minus the minimum of the equation 4 and is approximated by:

$$V_\sim = \frac{VI}{4\pi C_{HV} f V_0} \tag{5}$$

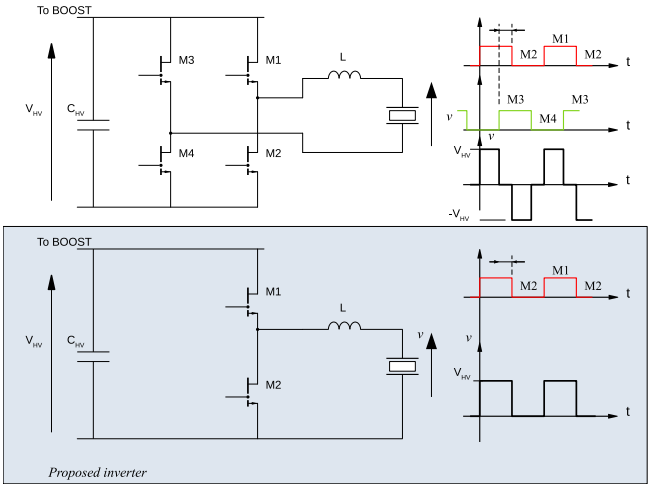

Fig. 4. Inverter topology: H bridge and corresponding waveforms (top); proposed design (bottom)

The value of C_{HV} is then calculated in order to limit the oscillation $V_{\sim}$ to a limit denoted ΔV, i.e. $V_{\sim} < \Delta V$. Taking into account 5 leads then to:

$$C_{HV} > \frac{VI}{4\pi f V_0 \Delta V} \tag{6}$$

C. Design of the inverter

The inverter converts the DC voltage of the HV bus into an AC voltage. For purpose of efficiency improvement, as well as practical implementation, the voltage v is not purely sinusoidal, but has a square waveform, its harmonics being filtered by the resonance of the tactile plate.

Classic implementations use H-Bridge converters, built with 4 MOSFETS that form the vertical bar of an H, while the load corresponds to the horizontal bar. By changing the polarity of the voltage across the load, an alternating supply voltage can be created. Moreover, by introducing a delay between the vertical MOSFETS, the fundamental of v can be set to a value, with a maximum equal to $\frac{4}{\pi}V_0$ (fig.4, top).

Because the voltage V_{HF} is modulated to form the haptic feedback, the controllability of the fundamental of v is not required in our proposed design. Therefore, to simplify the inverter, we consider using one leg only [12], which reduces the circuit complexity, but divides by 2 the fundamental of v which is then equal to $\frac{2}{\pi}V_0$ (fig.4, bottom); the equations 6 gives then:

$$C_{HV} > \frac{I}{2\pi^2 f \Delta V} \tag{7}$$

D. Equivalent electrical model of the inverter

With the proposed design, the capacitor C_{HV} temporarily stores the discharging energy of C_0 when V is decreasing, and feeds it back to C_0 when V increases. The value found in 7 will limit the resulting voltage ripple of V_{HV} to a value found to be acceptable. But this charging/discharging process of C_0 is transparent for the BOOST converter. It is therefore convenient to represent the behaviour of the inverter and its haptic surface in average over the the period $T = 1/f$ by an equivalent electrical circuit, that consume the same power. This is essential when choosing the haptic driver, because it has to be able to drive this equivalent load.

In our case, this equivalent electrical circuit is the capacitor C_{HV} in parallel with a resistor R_{eq} as described figure 5.

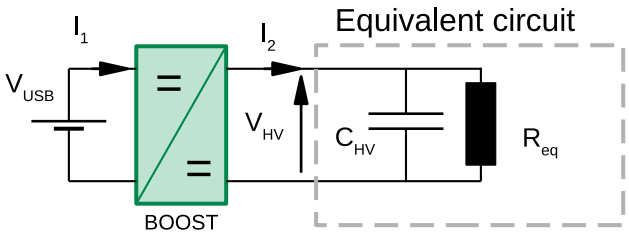

Fig. 5. Equivalent electrical circuit of the inverter.

If the plate is operated at the resonance frequency, the power consumption of the tactile plate is equal to $\frac{V^2}{2R_m}$, in average over the period $T = 1/f$. Hence, to calculate R_{eq}, we write:

$$\frac{V^2}{2R_m} = \frac{V_0^2}{R_{eq}} \tag{8}$$

leading to:

$$R_{eq} = 2\left(\frac{V_0}{V}\right)^2 R_m = 2\left(\frac{\pi}{2}\right)^2 R_m \tag{9}$$

Based on these design principles, an experimental validation of the proposed methodology is carried out.

III. Experimental results

A. System's description

A 165x123x2 mm^3 tactile plate was designed to produce friction reduction at 60 kHz. To actuate the plate, 19 piezoelectric actuators were bonded at the longer edge, all connected in parallel electrically. The plate requires a voltage $V = 25V$ and a current $I = 94mA$ to operate, while the power consumption is estimated to 0.5W at maximum vibration amplitude. An identification of the blocked capacitance of the tactile plate has been performed, and we have found $C_0 = 9nF$, $R_m = 625\Omega$, $C_m = 10.626pF$, $L_m = 0.6713H$. The resonance frequency is equal to $59589Hz$. A capacitance $C_{HV} = 150nF$ is then calculated with $\Delta V = 0.5V$ from the equation 7.

The driver was built around 2 GaN (Gallium Nitride) MOSFETS (GS66502B from GaN); they are found in small Surface Mount Package and small footprint, which leads to an easy integration. An inductor $L = 470\mu H$ was selected to reduce the inrush current. The MOSFETS are controlled by a micro-controller (Nucléo Board from STMicroelectronics), that includes a resonant frequency tracking algorithm to guarantee operations at resonance of the plate.

An evaluation board from Boréas (BOS1901-KIT) is chosen for the Haptic feedback. This board comes with a software that makes easy to program a sequence of haptic feedback. It is based on the BOS1901W which has a very small footprint

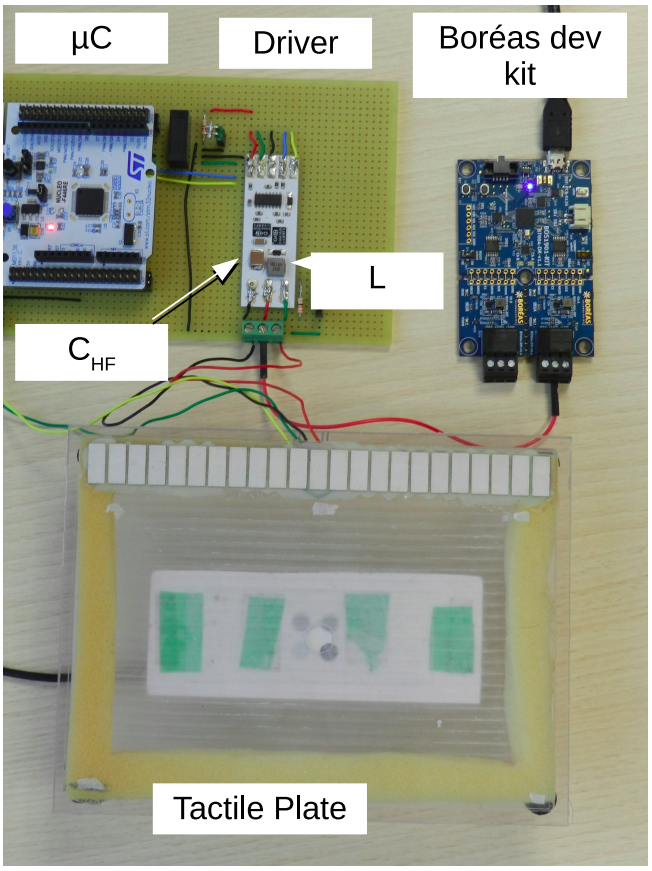

Fig. 6. Experimental setup used in the experiment.

$(4.5mm^2)$. A host PC running matlab (Mathworks) generates the modulation signal of V_{HV}, and sends it to the haptic driver through the USB port, using the Audio mode of the Boréas chip. We found from the equation 9 $R_{eq} = 3,2k\Omega$, which is drivable for the chip.

The plate is fixed on a force sensor (K3D40 from PM Instrumentation) in order to measure the friction reduction when a finger slides over it, with a sample time of $8ms$. Moreover, a current sensor (E27 from Metrix) allows to measure the current from the boost converter. Finally, the experimental setup is presented figure 6, on which experimental measurements were carried out to validate the approach, and which are presented in the next section.

B. Experimental measurements

1) Voltage ripple: To validate the calculation of C_{HV}, we have reported figure 7 the the voltage V_{HV} as a function of time with $V_0 = 12V$.

During this test, the voltage across the tactile plate has a square waveform at $f = 59655Hz$, from $V = 0V$ to $V = V_{HV}$, as expected from the behaviour of the half bridge and the plate. When V is increasing from $0V$ to V_{HV} (ie during a positive front), the capacitance C_{HV} discharge to the blocked capacitance of the tactile plate, and the voltage V_{HV} decreases from 11.83V to 11.25V, leading to an energy discharge $E =$

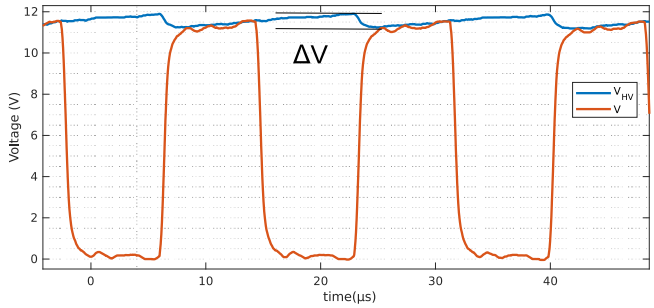

Fig. 7. Voltage V (red) and V_{HV} (blue) in the experimental test bench.

$1\mu J$ calculated from 1. If we compare this amount of energy to the energy E_0 actually stored into the blocked capacitance C_0 of the plate ($E_0 = 500\mu J$), we can conclude that the H bridge shows energy loss, reducing η, the efficiency of the conversion. As a result, the voltage ripple ΔV is increased: the expected value was 150mV at $V_{HV} = 12V$, and we obtained $580mV$. Taking into account η in the equation 3 leads to a revised value of ΔV:

$$\Delta V = \frac{I}{2\pi^2 f C_{HV} \eta} \tag{10}$$

In our device, we estimate then $\eta = 27\%$. The power losses also change the value of R_{eq}, because the power to the plate is smaller that the power supplied to the inverter. Therefore we write:

$$\frac{V^2}{2R_m} = \eta \frac{V_0^2}{R_{eq}} \tag{11}$$

leading to:

$$R_{eq} = 2\eta \left(\frac{V_0}{V}\right)^2 R_m \tag{12}$$

2) Haptic feedback: To validate that the Boost converter is able to dynamically drive the bus voltage V_{HV} in order to produce a programmable haptic feedback, we have defined a waveform that is strictly positive and which contains 2 harmonics, at the same amplitude, as follows:

$$w = W_m + \frac{W_0}{2}\left(1 + \frac{1}{2}sin(2\pi f_1 t) + \frac{1}{2}sin(2\pi f_2 t)\right) \tag{13}$$

By principle, the Boreas creates a voltage V_{HV} that is proportional to w, *i.e.* $V_{HV} = V_{MAX} \times w$ with V_{MAX} = 90V. The figure 8 shows the voltage V_{HV} as a function of time, with $W_0 = 0.25$, $W_m = 0.06$, $F_1 = 10Hz$ and $F_2 = 25Hz$.

The figure 8 demonstrates that the boost converter is able to dynamically drive the DC bus voltage. The voltage ripple ΔV is small with regard to V_{HV}. As a result, the vibration amplitude of the tactile plate varies with V_{HV}, and can produce a tactile feedback.

3) Assessment of the tactile feedback: To assess the haptic feedback that is produced by all the system, we measured the modulation of the friction force by the tactile plate, when programmed with the haptic driver. For this test, a user is

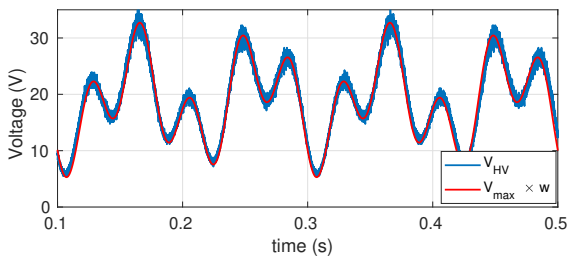

Fig. 8. Comparison between the reference value (red) for the bus voltage V_{HV} and its measurement (blue).

sliding his finger on the plate, while the DC bus voltage is modulated in the same way as presented figure 8. The user is asked to press with a constant force (around 0.3N). We record the lateral force F_y as depicted figure 9.

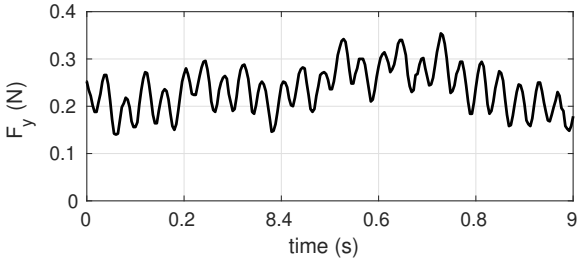

Fig. 9. Recorded lateral force F_y when the DC bus voltage V_{HF} is modulated according to the figure 8.

For the purpose of comparison, we calculated the Fast Fourrier Transform of F_y, depicted figure 10. We have also put on the same figure the two harmonics of the reference signal.

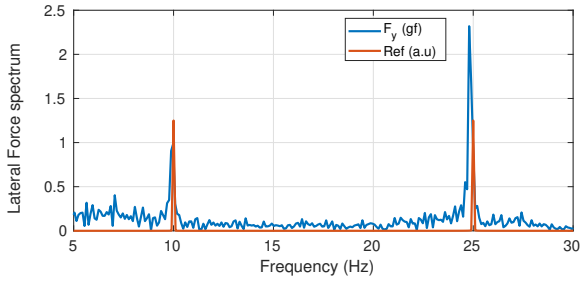

Fig. 10. Fast Fourrier Transform of the lateral force produced by the tactile plate, and comparison with the reference signal w.

The figure 10 clearly shows that both frequencies are present in the spectral content of the force F_y. However, even if the two harmonics of voltage have the same amplitude, it is not the case for the resulting force: 2.32 is the amplitude for the harmonic at 25Hz, and 0.98 for the harmonic at 10Hz all in arbitrary units. Viscoelastic properties of finger may be responsible of this difference [13]. Interestingly, the amplitude of the lateral force frequency components are approximately in the same ratio of the frequency (2.5). This result does not call into question the topology proposed in this paper, but questions the link between the supply voltage and the friction forces, which has always been assumed constant, and is outside the scope of this paper.

4) Energy consumption: We investigated the current that flows from the haptic driver to the inverter, for the reference of equation 6. First, we measured the current I_2 (see figure 1) for several values of V_{HV}, in steady state, as depicted figure 11.

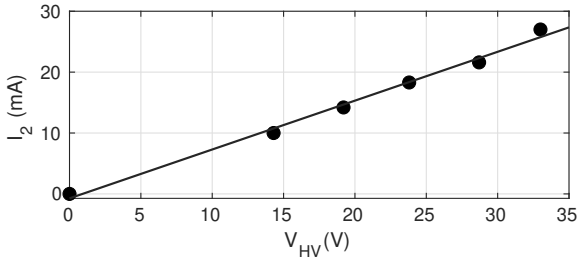

Fig. 11. Current I_2 flowing from the Boost converter as a function of the DC bus voltage.

On the figure 11, we also depict a linear fitting to the curve, which slope is equal to $0.802mA/V$. Given the model of section II-B, the value of R_{eq} is equal to the inverse of this slope, leading to $R_{eq} = 1207\Omega$. This value is larger than what is calculated from equation 9 (827Ω); an efficiency $\eta = 40\%$ would lead to the same value of equivalent resistor.

We then considered dynamic change of the voltage V_{HV}, in two cases:

- the inverter is not switching, so the the haptic driver only drive C_{HV},
- the inverter is switching, so the haptic driver also supply power to the tactile plate through the inverter.

We compare figure 12 the measurements to the output of the model for each case.

In the figure 12, the model is very close to the measurements, for both cases (with and without the inverter switching). We can conclude that the model describes well the behaviour of the inverter for the boost converter.

IV. Conclusion

This paper has presented a new driver topology that makes possible to use a commercial haptic driver to supply power to an ultrasonic tactile plate. The DC bus capacitor is used as a temporary energy storage that fills and empties the blocked capacitance of the piezoelectric actuators. With this design, a $4.5mm^2$ electronic circuit could drive a $200cm^2$ tactile plate. To reduce the size of the driver, we proposed an Half bridge that uses only 2 MOSFET transistors.

We have validated the design procedure, and introduced the efficiency of the converter into the calculation. We also have shown that the frequency content of the friction forces produced by the tactile plate follows the reference sent to the haptic driver, but also that the gain between the haptic signal and the friction forces depend on frequency. Finally, an

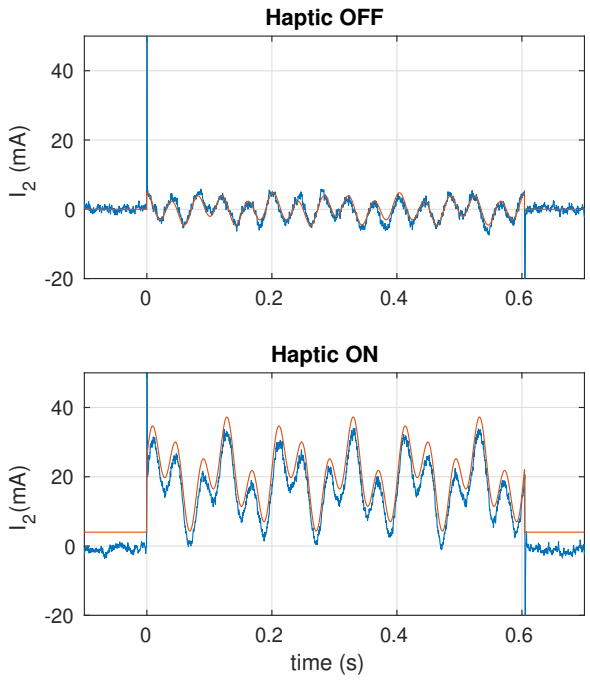

Fig. 12. Current I_2 flowing from the Boost converter in dynamic change of V_{HV}; measurements (blue) and model with $R_{eq} = 1207\Omega$ (red).

equivalent model of the inverter is proposed and validated by static and dynamic measurements.

Further work will try to improve the efficiency of the inverter, which is between 25% and 40%. Higher efficiency will reduce the power consumption of the system, a concern in handheld devices for example. Thanks to this topology, we extend the capabilities of commercial haptic drivers to the field of haptic surfaces. This will help to reduce the cost of their control electronic and to introduce more haptic surfaces into consumer products.

ACKNOWLEDGMENT

XXX

REFERENCES

[1] V. Hayward and K. E. Maclean, "Do it yourself haptics: part i," *IEEE Robotics & Automation Magazine*, vol. 14, no. 4, pp. 88–104, 2007.

[2] S. Choi and K. J. Kuchenbecker, "Vibrotactile display: Perception, technology, and applications," *Proceedings of the IEEE*, vol. 101, no. 9, pp. 2093–2104, 2013.

[3] S. Chaput, D. Brooks, and G.-Y. Wei, "A 3-to-5v input 100vpp output 57.7mw 0.42% thd+n highly integrated piezoelectric actuator driver," in *2017 IEEE International Solid-State Circuits Conference (ISSCC)*, 2017, pp. 360–361.

[4] C. Basdogan, F. Giraud, V. Levesque, and S. Choi, "A review of surface haptics: Enabling tactile effects on touch surfaces," *IEEE Transactions on Haptics*, vol. 13, no. 3, pp. 450–470, 2020.

[5] C. Shultz, M. Peshkin, and J. E. Colgate, "The application of tactile, audible, and ultrasonic forces to human fingertips using broadband electroadhesion," *IEEE Transactions on Haptics*, vol. 11, no. 2, pp. 279–290, 2018.

[6] E. Vezzoli, Z. Vidrih, V. Giamundo, B. Lemaire-Semail, F. Giraud, T. Rodic, D. Peric, and M. Adams, "Friction reduction through ultrasonic vibration part 1: Modelling intermittent contact," *IEEE Transactions on Haptics*, vol. 10, no. 2, pp. 196–207, 2017.

[7] Y. Rekik, E. Vezzoli, L. Grisoni, and F. Giraud, "Localized haptic texture: A rendering technique based on taxels for high density tactile feedback," ser. CHI '17. New York, NY, USA: Association for Computing Machinery, 2017, p. 5006–5015.

[8] M. Wiertlewski and J. E. Colgate, "Power optimization of ultrasonic friction-modulation tactile interfaces," *IEEE Transactions on Haptics*, vol. 8, no. 1, pp. 43–53, 2015.

[9] L. Winfield, J. Glassmire, J. E. Colgate, and M. Peshkin, "T-pad: Tactile pattern display through variable friction reduction," in *Second Joint EuroHaptics Conference and Symposium on Haptic Interfaces for Virtual Environment and Teleoperator Systems (WHC'07)*, 2007, pp. 421–426.

[10] F. Giraud, M. Amberg, B. Lemaire-Semail, and G. casiez, "Design of a transparent tactile stimulator," in *2012 IEEE Haptics Symposium (HAPTICS)*, 2012, pp. 485–489.

[11] M. Schmid, E. Benes, W. Burger, and V. Kravchenko, "Motional capacitance of layered piezoelectric thickness-mode resonators," *IEEE Transactions on Ultrasonics, Ferroelectrics, and Frequency Control*, vol. 38, no. 3, pp. 199–206, 1991.

[12] O. Lucia, J. M. Burdio, I. Millan, J. Acero, and D. Puyal, "Load-adaptive control algorithm of half-bridge series resonant inverter for domestic induction heating," *IEEE Transactions on Industrial Electronics*, vol. 56, no. 8, pp. 3106–3116, 2009.

[13] M. K. Saleem, C. Yilmaz, and C. Basdogan, "Psychophysical evaluation of change in friction on an ultrasonically-actuated touchscreen," *IEEE Transactions on Haptics*, vol. 11, no. 4, pp. 599–610, 2018.